DALTON

Synthesis and characterisation of hexaruthenium carbido carbonyl clusters containing arenes derived from biphenyl

Brian F. G. Johnson,*[a] Douglas S. Shephard,[a] Dario Braga,[b] Fabrizia Grepioni*[b] and Simon Parsons[c]

[a] *Department of Chemistry, The University of Cambridge, Lensfield Rd., Cambridge, UK CB2 1EW*
[b] *Dipartimento di Chemica 'G. Ciamician', dell'Università di Bologna, Via Selmi 2, 40126 Bologna, Italy*
[c] *Department of Chemistry, The University of Edinburgh, West Mains Road, Edinburgh, UK EH9 3JJ*

Several hexaruthenium carbido clusters $[Ru_6C(CO)_{14}(\eta^6\text{-}C_6H_5C_6H_4Me)]$ **1a**, $[Ru_6C(CO)_{14}(\eta^6\text{-}MeC_6H_4C_6H_5)]$ **1b**, $[Ru_6C(CO)_{14}(\eta^6\text{-}C_6H_5C_6H_4Et)]$ **2a**, $[Ru_6C(CO)_{14}(\eta^6\text{-}EtC_6H_4C_6H_5)]$ **2b**, $[Ru_6C(CO)_{14}(\eta^6\text{-}C_6H_5C_6H_4Ph)]$ **3** and $[Ru_6C(CO)_{14}(\eta^6\text{-}C_6H_5C_6H_3Ph_2)]$ **4** have been synthesized by the reaction of triruthenium dodecacarbonyl and the appropriate polycyclic hydrocarbon. The compounds have been fully characterised by a variety of methods including single-crystal X-ray diffraction for **1a**, **1b** and **2b**. The supramolecular architectures of these three solid-state structures have also been examined. Selectivity of the cluster build-up reaction at different aryl sites is discussed.

We have previously shown that hexaruthenium carbido cluster build-up at a single arene site is favoured with respect to polyphenyl hydrocarbon ligands in which the aryl rings are identical.[1] The question was then posed: which product would be formed if the steric/electronic character of the two arene rings was different? We have also observed that in the series of simple benzene derivatives benzene, toluene, *m*-xylene, mesitylene the yield of the Ru_6C(arene) is related to the number of methyl substituents, mesitylene giving the largest.[2] However due to the nature of the preparative conditions, the arene being both ligand and thermolysis solvent, it is not possible to separate the effect of temperature and that of the steric/electronic character of the arene. Therefore a set of simple experiments was devised to help determine the factors governing the aryl site of choice and hence any selectivity inherent in this classic cluster reaction.

Results and Discussion

The aromatics chosen were 4-phenyltoluene, 4-ethylbiphenyl, 1,4-diphenylbenzene and 1,3,5-triphenylbenzene. The four Ru_6C derivatives **1–4** were prepared from the reaction of $[Ru_3(CO)_{12}]$ with either an excess or a 0.5 molar quantity of the appropriate polyarene in *n*-octane under reflux. In all cases the reaction proceeded to give moderate yields of a single product together with small amounts of $[Ru_6C(CO)_{17}]$. No evidence was found for the production of hydrocarbon-linked clusters. The cluster compounds were purified by TLC on silica plates, using an eluent based on dichloromethane–hexane (30:70). Crystals of **1** and **2** suitable for structure determination were nucleated from dichloromethane–pentane by slow diffusion.

The 4-phenyltoluene isomeric derivatives **1a** and **1b** were observed as a single well defined red-brown band on the TLC plate. The IR spectrum in the CO region was consistent with that of a Ru_6C(arene) compound bound in an η^6 mode. The FAB mass spectrum showed a single molecular ion peak at *m/z* 1178 (calc. 1178), and the loss of several CO units. A ^1H NMR spectrum in $CDCl_3$ at ambient conditions showed a mixture of the two co-ordination isomers. However, because of the difficulty in separating isomers **1a** and **1b** a variable-temperature NMR experiment was undertaken to determine whether or not an equilibrium/conversion process was present. The solvent used was 1,1,2,2-tetrachloro[$^2H_2$]ethane so higher temperatures could be reached without solvent-loss problems. The experimental procedure involved collecting data at 20 K intervals from ambient temperature to a maximum of 400 K. At each temperature increment the sample/apparatus was given 30 min to reach thermal equilibrium. The spectroscopic evidence thus gained showed no change in isomer ratio with temperature and therefore no measurable interconversion over the time of the experiment. To distinguish the resonances due to the specific isomers a series of nuclear Overhauser effect experiments were undertaken. This type of experiment has a second line of interest. If interconversion were occurring between the two isomeric forms on the double resonance time-scale then we should have seen mutual saturation of the two corresponding signals. It was also noticed that solutions made up from different crops of crystals analysed by NMR spectroscopy gave varied isomer ratios. This is at odds with the solid-state structure of **1** which contains both isomers in equal proportions (see below) and implies that ad-crystallisation occurs alongside co-crystallisation.

Solid-state molecular structures of $[Ru_6C(CO)_{14}(\eta^6\text{-}C_6H_5C_6H_4\text{-}Me)]$ 1a and $[Ru_6C(CO)_{14}(\eta^6\text{-}MeC_6H_4C_6H_5)]$ 1b

The solid-state molecular structure of the isomeric Ru_6C(arene) compounds **1a** and **1b** are shown in Figs. 1 and 2 and important structural parameters are given in Table 1. The two isomers, co-crystallised from dichloromethane solution, are closely related and shall be discussed together. This serendipitous self-assembly of the two co-ordination isomers allows very close comparison to be made. Both **1a** and **1b** contain a $Ru_6C(CO)_{14}$ unit attached to the biphenyl derivative in an η^6 mode in keeping with other arene clusters previously characterised. In **1a** the cluster is bound to the phenyl (C_6H_5) part of the ligand, whilst in **1b** it co-ordinates the tolyl ($C_6H_4CH_3$) ring. The hexaruthenium cluster core of each isomer encapsulates a carbido atom at the centre. In both **1a** and **1b** the interstitial atom is bound closest to the ruthenium atom carrying the arene ligand. The metal–metal distances in each isomer give a similar range

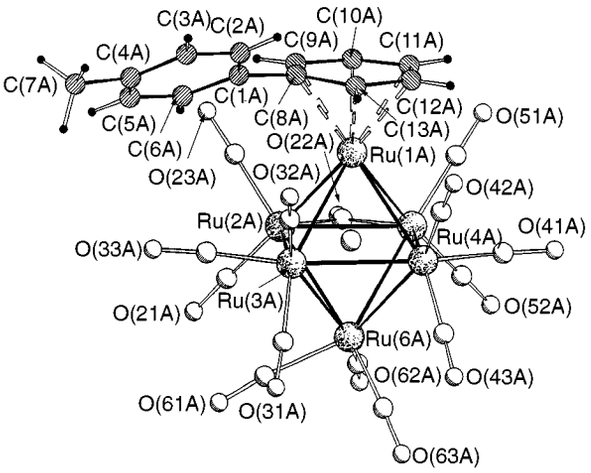

Fig. 1 Solid-state molecular structure of compound **1a**, showing the atomic labelling scheme; the C atoms of the CO groups bear the same numbering as those of the corresponding O atoms

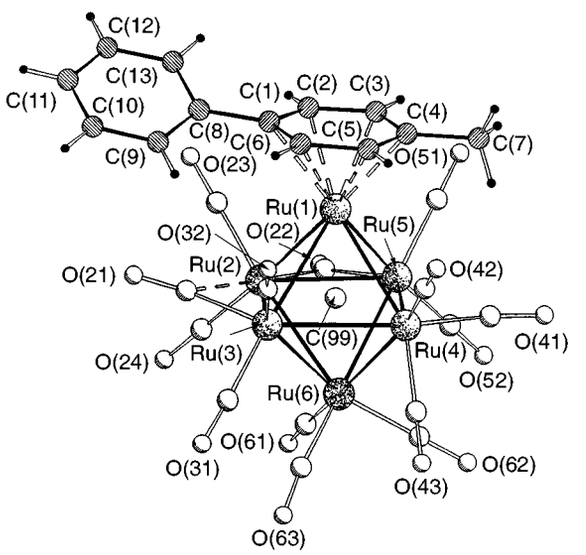

Fig. 2 Solid-state molecular structure of compound **1b**. Details as in Fig. 1

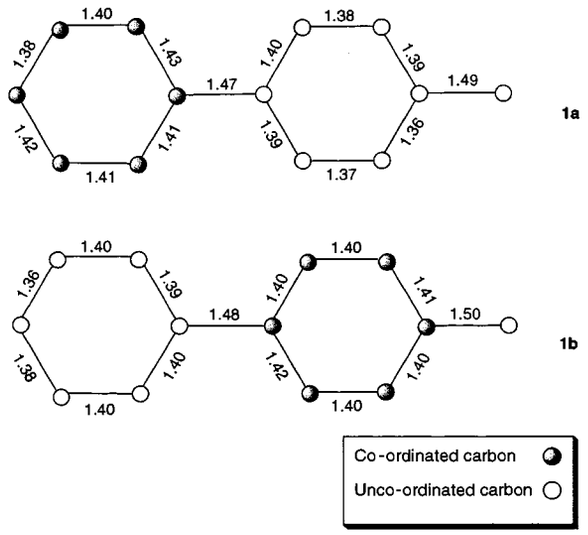

Fig. 3 Representation of the C–C bonds in compounds **1a** and **1b**; distances in Å as projected from above the molecules

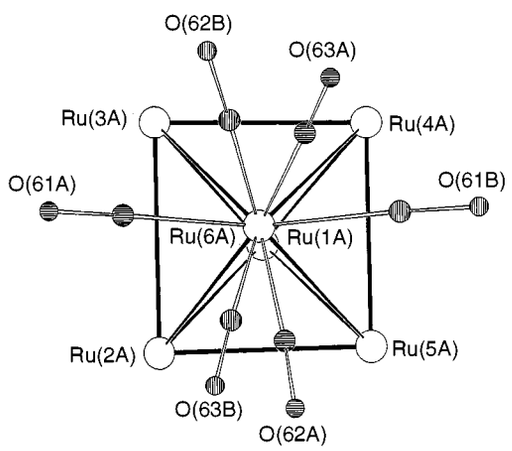

Fig. 4 Disorder displayed by the Ru(6A) tricarbonyl group in compound **1a**. The two orientations are related by a 180° rotation perpendicular to the plane of the figure

[Ru(4)–Ru(6) 2.832(2) to Ru(4)–Ru(5) 3.061(2) for **1b** and Ru(2A)–Ru(5A) 2.834(2) to Ru(2A)–Ru(3A) 3.044(2) Å for **1a**]. The carbonyl-bridged metal–metal contacts are among the shortest in each isomer.

The arene–cluster bonding in both isomers **1a** and **1b** shows a distinct pattern of five short and one long metal–carbon distance. The long Ru–C_{arene} bond in each isomer is between the apical ruthenium atom and the ring carbon bound to the pendant phenyl ring [Ru(1A)–C(8A) 2.32(1) in **1a** and Ru(1)–C(1) 2.31(1) Å in **1b**], whilst the remaining five distances are identical within estimated error. The C–C distances in the hydrocarbon frameworks in both **1a** and **1b** are given in Fig. 3. It is of interest how little the bond lengths vary between the co-ordinated and unco-ordinated rings in these structures. Communication between the phenyl rings, shown to occur by NMR spectroscopy, is likely to be related to the inter-ring distances and the torsion angles. Both **1a** and **1b** show an inter-ring bond length less than that normally associated with a C–C single bond (see Fig. 3), whilst they give torsion angles of 34 and 21° respectively. All the C_6 rings in **1a** and **1b** are planar within estimated error.

The remaining co-ordination sphere of the cluster **1a** is made up of thirteen terminal carbonyl ligands and a bridging CO triangulating the Ru(2A)–Ru(5A) vector. The Ru(6A) tricarbonyl group is systematically disordered about its rotation axis and is shown in Fig. 4. The disordered COs interlock with a second molecule of **1a** related by a centre of inversion. Hence the co-ordination isomer **1a** is divided equally between two rotamers in the solid state. This is just one of many interesting intermolecular interactions displayed in this co-crystal which are discussed below. The carbonyl polyhedron of **1b** is made up of twelve terminal carbonyl ligands, together with a bridging CO triangulating the Ru(2)–Ru(5) vector and a semi-bridging CO predominantly bound to Ru(3) with a secondary interaction to Ru(2).

Solid-state supramolecular architecture. The solid-state supramolecular architecture of the crystal **1a**/**1b** shows many interesting intermolecular interactions as well as the disordered CO interlocking in **1a** previously mentioned. Fig. 5 shows an overall packing diagram for the **1a**/**1b** crystal. Packing occurs in such a manner as to maximise CO···OC and arene–arene interactions, as previously observed in bis(arene) hexaruthenium clusters. Molecular pairing through arene–arene interactions of the **1a**···**1a** and **1b**···**1b** type dominate. These 'graphitic' like interactions between the substituted biphenyl ligands are shown in Figs. 6 and 7 respectively. The distance between the parallel toluene planes in both types of interaction is 4.3 Å even though the two interactions are quite topologically different. The figures show how the aryl pairing is more efficient in **1b** than in **1a**.

Along with these arene–arene interactions are a series of interesting intermolecular interactions of the CO···H–C type.

Table 1 Selected bond distances (Å)

Compound **1a**

Ru(5A)–C(51A)	1.870(9)	Ru(5A)–C(52A)	1.874(9)	Ru(5A)–C(22A)	2.044(8)
Ru(5A)–C(99A)	2.087(7)	Ru(5A)–Ru(2A)	2.8338(14)	Ru(5A)–Ru(1A)	2.8826(12)
Ru(5A)–Ru(6A)	2.884(2)	Ru(5A)–Ru(4A)	2.9586(14)	Ru(1A)–C(99A)	1.912(7)
Ru(1A)–C(10A)	2.210(8)	Ru(1A)–C(13A)	2.234(8)	Ru(1A)–C(9A)	2.242(8)
Ru(1A)–C(11A)	2.250(9)	Ru(1A)–C(12A)	2.254(9)	Ru(1A)–C(8A)	2.312(7)
Ru(1A)–Ru(4A)	2.8505(12)	Ru(1A)–Ru(3A)	2.871(2)	Ru(1A)–Ru(2A)	2.874(2)
Ru(2A)–C(21A)	1.873(9)	Ru(2A)–C(23A)	1.899(8)	Ru(2A)–C(22A)	2.050(8)
Ru(2A)–C(99A)	2.068(7)	Ru(2A)–Ru(6A)	2.8657(12)	Ru(2A)–Ru(3A)	3.0438(13)
Ru(3A)–C(42A)	1.889(11)	Ru(3A)–C(32A)	1.894(10)	Ru(3A)–C(31A)	1.91(2)
Ru(3A)–C(34A)	1.92(2)	Ru(3A)–C(99A)	2.050(7)	Ru(3A)–Ru(4A)	2.829(2)
Ru(3A)–Ru(6A)	2.8637(13)	Ru(6A)–C(56A)	1.77(2)	Ru(6A)–C(55A)	1.80(2)
Ru(6A)–C(63A)	1.91(3)	Ru(6A)–C(62A)	1.95(3)	Ru(6A)–C(61A)	1.99(2)
Ru(6A)–C(54A)	2.05(2)	Ru(6A)–C(99A)	2.087(7)	Ru(6A)–Ru(4A)	2.892(2)
Ru(4A)–C(43A)	1.859(13)	Ru(4A)–C(42A)	1.874(10)	Ru(4A)–C(41A)	1.905(12)
Ru(4A)–C(99A)	2.056(7)	C(8A)–C(9A)	1.414(12)	C(8A)–C(13A)	1.417(12)
C(8A)–C(1A)	1.479(11)	C(9A)–C(10A)	1.408(12)	C(10A)–C(11A)	1.42(2)
C(11A)–C(12A)	1.39(2)	C(12A)–C(13A)	1.397(13)	C(1A)–C(6A)	1.379(10)
C(1A)–C(2A)	1.395(10)	C(2A)–C(3A)	1.378(12)	C(3A)–C(4A)	1.386(12)
C(4A)–C(5A)	1.381(11)	C(4A)–C(7A)	1.492(11)	C(5A)–C(6A)	1.375(11)
C(22A)–O(22A)	1.173(9)	C(51A)–O(51A)	1.157(10)	C(52A)–O(52A)	1.146(10)
C(32A)–O(23A)	1.130(9)	C(21A)–O(21A)	1.143(9)	C(32A)–O(32A)	1.147(10)
C(42A)–O(33A)	1.145(11)	C(31A)–O(31A)	1.14(2)	C(34A)–O(34A)	1.19(3)
C(61A)–O(61A)	1.14(2)	C(62A)–O(62A)	1.11(3)	C(63A)–O(63A)	1.08(3)
O(63A)–O(55A)	1.74(2)	C(54A)–O(54A)	1.18(3)	C(55A)–O(55A)	1.24(2)
C(56A)–O(56A)	1.16(2)	C(42A)–O(42A)	1.135(11)	C(41A)–O(41A)	1.157(12)
C(43A)–O(43A)	1.169(14)				

Compound **1b**

Ru(5)–C(52)	1.875(7)	Ru(5)–C(51)	1.892(8)	Ru(5)–C(22)	2.039(8)
Ru(5)–C(99)	2.061(7)	Ru(5)–Ru(6)	2.8328(13)	Ru(5)–Ru(2)	2.8421(11)
Ru(5)–Ru(1)	2.893(2)	Ru(5)–Ru(4)	3.0609(14)	Ru(1)–C(99)	1.927(7)
Ru(1)–C(5)	2.225(8)	Ru(1)–C(4)	2.231(8)	Ru(1)–C(3)	2.240(7)
Ru(1)–C(2)	2.240(8)	Ru(1)–C(6)	2.254(7)	Ru(1)–C(1)	2.312(7)
Ru(1)–Ru(3)	2.8642(13)	Ru(1)–Ru(4)	2.8726(13)	Ru(1)–Ru(2)	2.8951(12)
Ru(6)–C(62)	1.896(9)	Ru(6)–C(61)	1.911(10)	Ru(6)–C(63)	1.916(8)
Ru(6)–C(99)	2.096(7)	Ru(6)–Ru(4)	2.8325(13)	Ru(6)–Ru(2)	2.9185(13)
Ru(6)–Ru(3)	2.927(2)	Ru(2)–C(24)	1.882(8)	Ru(2)–C(23)	1.887(8)
Ru(2)–C(99)	2.069(7)	Ru(2)–C(22)	2.098(7)	Ru(2)–C(21)	2.491(8)
Ru(2)–Ru(6)	2.8654(14)	Ru(4)–C(43)	1.889(10)	Ru(4)–C(42)	1.901(10)
Ru(4)–C(41)	1.910(9)	Ru(4)–C(99)	2.055(7)	Ru(4)–Ru(3)	2.8757(12)
Ru(3)–C(32)	1.866(9)	Ru(3)–C(31)	1.907(9)	Ru(3)–C(21)	1.977(8)
Ru(3)–C(99)	2.061(7)	C(1)–C(2)	1.394(10)	C(1)–C(6)	1.421(11)
C(1)–C(1′)	1.486(11)	C(2)–C(3)	1.398(11)	C(3)–C(4)	1.414(12)
C(4)–C(5)	1.399(12)	C(4)–C(7)	1.500(11)	C(5)–C(6)	1.404(12)
C(8)–C(9)	1.396(11)	C(9)–C(10)	1.398(12)	C(10)–C(11)	1.381(13)
C(11)–C(12)	1.362(13)	C(12)–C(13)	1.395(12)	C(51)–O(51)	1.140(9)
C(52)–O(52)	1.145(8)	C(61)–O(61)	1.137(10)	C(62)–O(62)	1.144(9)
C(63)–O(63)	1.128(9)	C(24)–O(24)	1.142(8)	C(23)–O(23)	1.140(8)
C(22)–O(22)	1.172(8)	C(41)–O(41)	1.145(9)	C(42)–O(42)	1.139(11)
C(43)–O(43)	1.142(10)	C(21)–O(21)	1.140(9)	C(31)–O(31)	1.147(9)
C(32)–O(32)	1.146(10)				

Molecular pairing of compound **1a** by a very short CO · · · H–C interaction (2.249 Å) is shown in Fig. 8. By way of symmetry the interaction occurs twice between the molecular pair and is between an oxygen of a bridging carbonyl and that of a co-ordinated arene hydrogen. It has previously been postulated that the μ-COs of a given transition-metal carbonyl compound will be the most basic.[3] Also the co-ordination of arene compounds is known to increase the acidity of the aryl hydrogens. These two factors may promote CO · · · H–C type interactions. Further interactions of this type up to 2.60 Å are given in Table 2. The nature of this interaction is unclear although an admixture of dipole–dipole and hydrogen-bonding interactions may serve as an adequate description.

The utilisation of the substituted 4-methylbiphenyl appears to show little or no control over the co-ordination of the cluster to a particular arene ring. This is perhaps unsurprising on electronic grounds due to the small Hammett parameter associated with the substituent group. Steric hindrance due to the extra methyl group in the *para* position is small especially in the apical co-ordination site however it may still be anticipated to have an effect on the product distribution. Since none is detected, it is perhaps likely that the small degree to which the Me group sterically hinders the co-ordination at the arene is compensated for by the small +I effect and consequent increase in electron density in the doubly substituted ring.

Synthesis and characterisation of $[Ru_6C(CO)_{14}(\eta^6\text{-}C_6H_5C_6H_4\text{-}Et)]$ 2a and $[Ru_6C(CO)_{14}(\eta^6\text{-}EtC_6H_4C_6H_5)]$ 2b

The 4-ethylbiphenyl isomeric derivatives **2a** and **2b** were also isolated as a single red-brown band on the TLC plate. The IR spectrum in the CO region was consistent with that of a Ru_6C(arene) compound bound in an η^6 mode. The FAB mass spectrum showed a single molecular ion peak at *m/z* 1193 (calc. 1193), with a carbonyl regression consistent with these systems, showing the loss of several CO units. Proton NMR spectroscopy in $CDCl_3$ under ambient conditions showed a mixture of the two co-ordination isomers, although in this case the ratio of the isomers (≈20 : 1) was heavily biased towards **2a** (*i.e.* co-ordination to the C_6H_5 ring). This excess indicates that **2a** is the

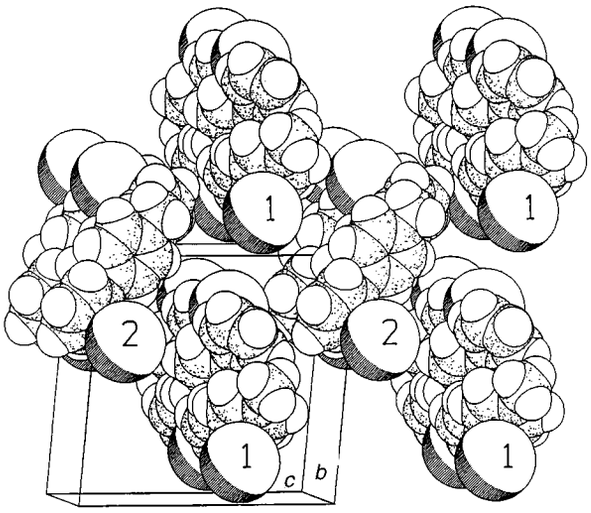

Fig. 5 Solid-state architecture of compound **1**. Carbonyls have been removed for clarity and cluster cores are represented by spheres positioned by their centre of mass

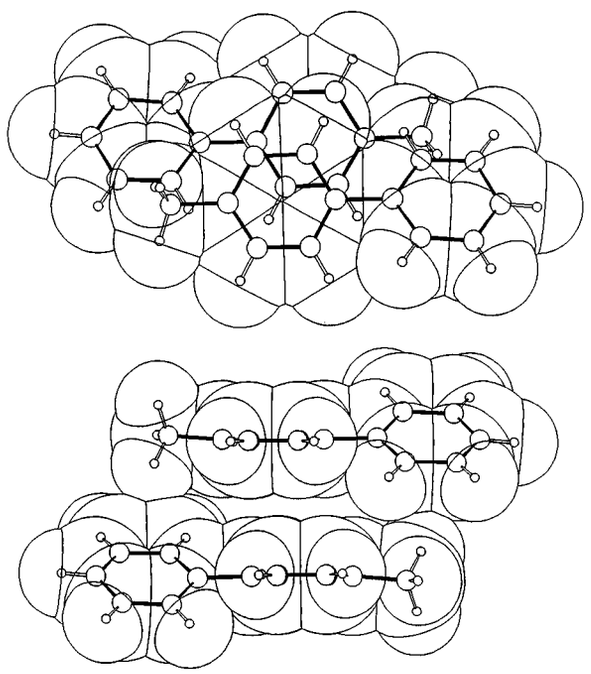

Fig. 6 'Graphitic' like interactions between the 4-methylbiphenyl aromatics in compound **1a**

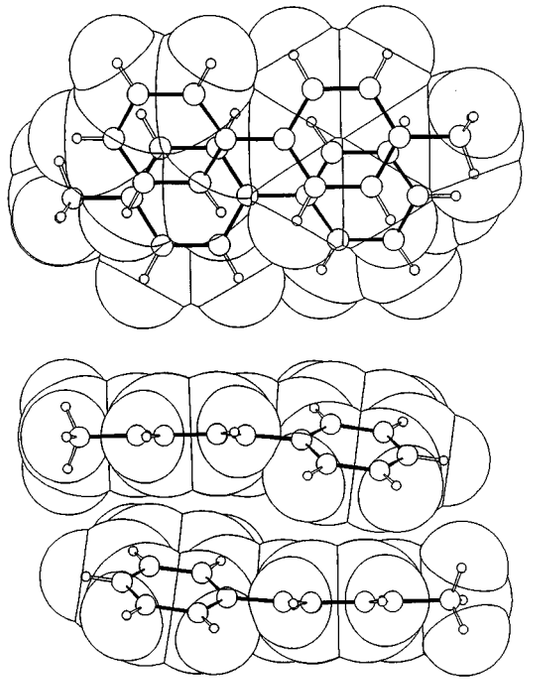

Fig. 7 'Graphitic' like interactions between the 4-methylbiphenyl aromatics in compound **1b**

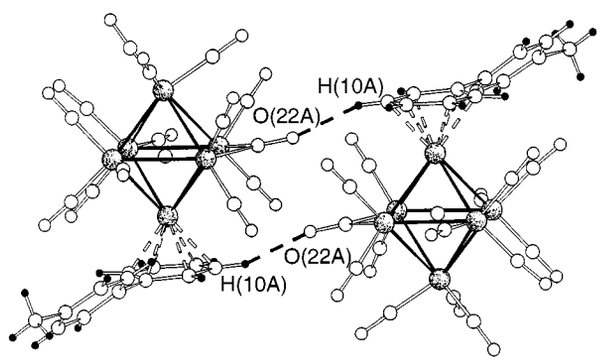

Fig. 8 The CO · · · H–C type interactions between molecules of compound **1a**

preferred product, presumably on kinetic grounds since whilst the Et group has a very small Hammett parameter it possesses a significant steric influence. Hence it is possible to exercise control over the product distribution of co-ordination isomers by careful choice of aryl substituent. This idea is extended in the synthesis of **3** and **4** where absolute control is encountered (see below).

The solid-state molecular structure of the minor isomer **2b** is shown in Fig. 9 along with selected structural parameters in Table 3. The molecular structure shows many strong similarities to **1b**. First, the migration of the interstitial carbon atom toward the ruthenium atom carrying the substituted biphenyl ligand gives an almost identical distance [Ru(1)–C(99) 1.94(1) Å]. Secondly, the cluster–arene bonding shows the same pattern of five short bonds and one long bond from the apical ruthenium to the ring carbon bound to the pendant phenyl group [Ru(1)–C(1) 2.30(1) Å]. Thirdly, the distribution of Ru–Ru bonds is very similar. Fourthly, the slight shortening of the inter-ring C–C distances is also apparent, again suggesting a degree of delocalisation across the ring π systems. The torsion angle between the rings is however much larger (43.7°). The Et group occupies a position above and away from the cluster core and both C–C bond lengths are consistent with those of single character. Thirteen terminal carbonyls and a μ-CO triangulating the Ru(4)–Ru(5) vector make up the remaining co-ordination sphere of the cluster core.

Solid-state supramolecular architecture of compound 2b. The solid-state architecture of compound **2b** also shows similar intermolecular interactions to those observed in **1a** and **1b** (Fig. 10). Again, on first inspection, the solid-state packing appears to maximise both CO · · · OC and arene–arene interactions. The 'graphitic' like arene–arene molecular pairing is subtly different however, possibly due to the steric hindrance of the Et group. As mentioned previously the torsion angle is greater in **2b** than in **1a** or **1b**. This produces an arene–arene interaction whereby a hydrogen atom in the 3 position points into the centre of the π orbitals of an adjacent ring (Fig. 11). Arene–arene interactions of this type have been previously documented in other solid-state systems.[4,5] Compound **2b** also shows molecular pairing due to an interaction of the CO · · · H–C type as observed in **1b**. Similar to **1b** the oxygen acceptor atom is part of a μ-CO and interacts with a hydrogen bound to a co-ordinated arene [O(42) · · · H(6)–C(6) 2.315 Å] to give a kind of 'dimer' (Fig. 12).

Synthesis and characterisation of $[Ru_6C(CO)_{14}(\eta^6\text{-}C_6H_5C_6H_4\text{-}Ph)]$ 3 and $[Ru_6C(CO)_{14}(\eta^6\text{-}C_6H_5C_6H_3Ph_2)]$ 4

Two further aryl ligands were used to make aryl derivatives, namely terphenyl (PhC_6H_4Ph) and 1,3,5-triphenylbenzene ($C_6H_3Ph_3$). The ^{1}H NMR spectrum of compound **3** in $CDCl_3$ indicated that a single isomer was produced in the thermolysis reaction, co-ordinated through a pendant phenyl group. The IR spectrum in the CO region was consistent with that of a Ru_6C(arene) compound bound in an η^6 mode. The positive-ion FAB mass spectrum showed a molecular ion peak at *m/z* 1242 (calc. 1241), with a carbonyl regression consistent with these systems, showing the loss of several CO units. This evidence indicates the ligand has remained intact during the reaction and a proposed molecular structure is given in Fig. 13. The solid-state structure of the co-ordination isomer, synthesized by a different route, has been determined.[6]

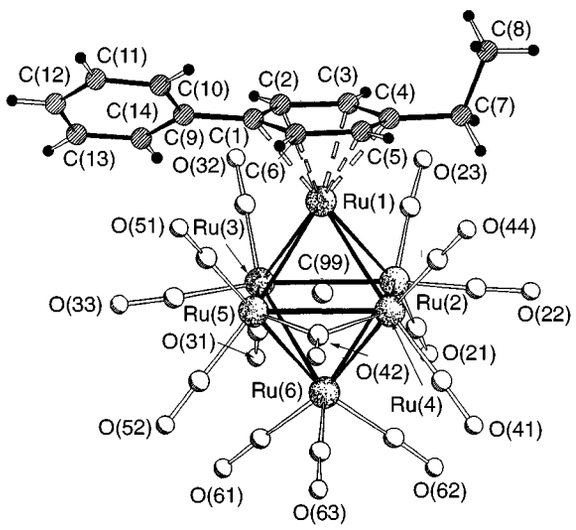

Fig. 9 Solid-state molecular structure of compound **2b**. Details as in Fig. 1

Table 2 The CO···H–C type interactions <2.60 Å between molecules of compounds **1a** and **1b**; C–H bonds are normalised to 1.08 Å

Donor	H	Acceptor	D···A/Å	H···A/Å	D–H···A/°
C(7)	H(7)	O(41)	3.384	2.386	152.9
C(9)	H(9)	O(33)	3.343	2.579	127.1
C(13)	H(13)	O(21)	3.459	2.383	174.1
C(5A)	H(5A)	O(24A)	3.336	2.566	127.6
C(7A)	H(7A1)	O(52A)	3.542	2.475	169.2
C(7A)	H(7A2)	O(22A)	3.474	2.574	140.3
C(10A)	H(10A)	O(22A)	3.283	2.249	159.7
C(12A)	H(12A)	O(63A)	3.027	2.552	103.6
C(13A)	H(13A)	O(43A)	3.204	2.385	131.4

The ^{1}H NMR spectrum of compound **4** in $CDCl_3$ also indicated that a single isomer was produced in the thermolysis reaction, co-ordinated through a pendant phenyl group. The IR spectrum in the CO region was consistent with that of a Ru_6C(arene) compound bound in an η^6 mode. The positive-ion FAB mass spectrum showed a molecular ion peak at *m/z* 1319 (calc. 1317), with a carbonyl regression consistent with these systems, showing the loss of several CO units. This evidence indicates the ligand has remained intact during the reaction and a proposed molecular structure is given in Fig. 14.

Conclusion

From these results it may be concluded that cluster build-up may only occur at an aryl ring that is suitably unhindered. However in the synthesis of compounds **3** and **4** it must be remembered that since there are more pendant phenyls than

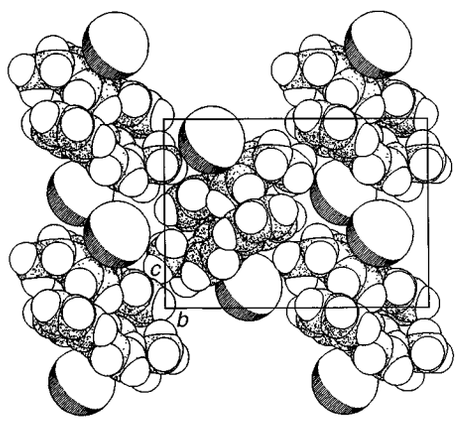

Fig. 10 Solid-state architecture of compound **2b**. Details as in Fig. 5

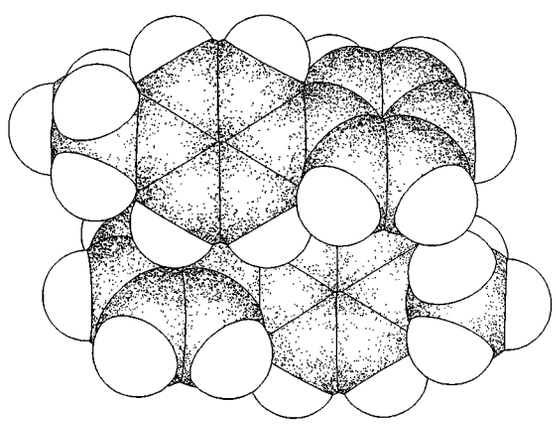

Fig. 11 Arene–arene interactions between the 4-ethylbiphenyl aromatics in compound **2b**

Table 3 Relevant bond distances (Å) for compound **2b**

Ru(1)–Ru(2)	2.879(2)	Ru(1)–Ru(3)	2.892(1)	Ru(1)–Ru(4)	2.893(3)
Ru(1)–Ru(5)	2.870(2)	Ru(2)–Ru(3)	2.831(2)	Ru(2)–Ru(4)	2.938(2)
Ru(2)–Ru(6)	2.905(2)	Ru(3)–Ru(5)	3.014(2)	Ru(3)–Ru(6)	2.889(2)
Ru(4)–Ru(5)	2.859(2)	Ru(4)–Ru(6)	2.854(2)	Ru(5)–Ru(6)	2.855(2)
Ru(1)–C(99)	1.94(1)	Ru(2)–C(99)	2.07(1)	Ru(3)–C(99)	2.06(1)
Ru(4)–C(99)	2.06(1)	Ru(5)–C(99)	2.04(1)	Ru(6)–C(99)	2.09(1)
Ru(1)–C(1)	2.30(1)	Ru(1)–C(2)	2.25(1)	Ru(1)–C(3)	2.25(1)
Ru(1)–C(4)	2.24(1)	Ru(1)–C(5)	2.25(1)	Ru(1)–C(6)	2.24(1)
C(1)–C(2)	1.42(2)	C(1)–C(6)	1.41(2)	C(1)–C(9)	1.48(2)
C(2)–C(3)	1.43(2)	C(3)–C(4)	1.40(2)	C(4)–C(5)	1.40(2)
C(5)–C(6)	1.39(2)	C(4)–C(7)	1.53(2)	C(7)–C(8)	1.53(2)
C(9)–C(14)	1.37(2)	C(9)–C(10)	1.39(2)	C(10)–C(11)	1.38(2)
C(11)–C(12)	1.34(2)	C(12)–C(13)	1.41(2)	C(13)–C(14)	1.38(2)
$C–O_{av}$	1.16(2)				

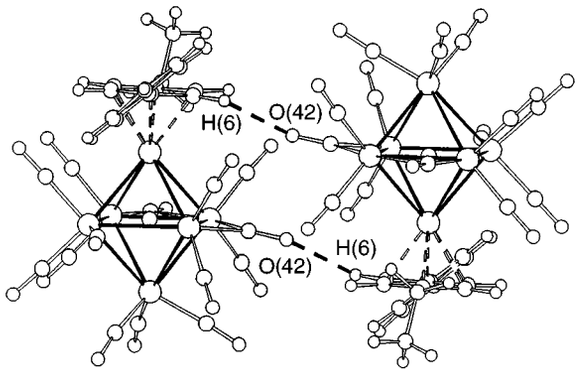

Fig. 12 The CO · · · H–C type interactions between molecules of compound **2b**

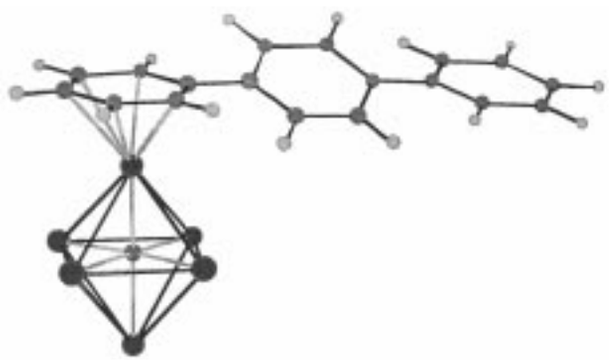

Fig. 13 Proposed molecular structure of compound **3**; the COs have been omitted for clarity

sterically hindered rings there is a statistical bias toward the coordination behaviour observed. The subtle electronic differences between the aryl rings in various experiments tend to suggest that electron-rich arenes are favoured although further examples are needed to confirm this.

We further conclude that when attempting to engineer solid-state arene cluster species, in which communication may occur across π contacts, the precise nature of the arene is of great importance to the supramolecular architecture produced. The construction of these organometal networks is our continuing goal.

Experimental

General

All reactions were carried out with the exclusion of air using solvents freshly distilled under an atmosphere of nitrogen. Subsequent work-up of products was achieved without precautions to exclude air. Infrared spectra were recorded on a Perkin-Elmer 1600 series FTIR spectrometer in CH_2Cl_2 using NaCl cells, positive-ion fast atom bombardment mass spectra using a Kratos MS50TC spectrometer using CsI as calibrant and ^{1}H NMR spectra in $CDCl_3$ using a Bruker 360B MHz instrument, referenced to internal $SiMe_4$. Separation of products was accomplished with Merck thin-layer chromatography (TLC) plates as supplied (0.25 mm layer of Kieselgel 60 F_{254}). The compound $[Ru_3(CO)_{12}]$ was prepared by the literature procedure.[7] 4-Methylbiphenyl, 4-ethylbiphenyl, terphenyl, 1,3,5-triphenylbenzene and *n*-octane from Aldrich Chemicals were used without further purification.

Synthesis and characterisation of $[Ru_6C(CO)_{14}(\eta^6\text{-}C_6H_5C_6H_4\text{-}Me)]$ 1a, 1b, $[Ru_6C(CO)_{14}(\eta^6\text{-}C_6H_5C_6H_4Et)]$ 2, $[Ru_6C(CO)_{14}(\eta^6\text{-}C_6H_5C_6H_4Ph)]$ 3 and $[Ru_6C(CO)_{14}(\eta^6\text{-}C_6H_5C_6H_3Ph_2)]$ 4

The compound $[Ru_3(CO)_{12}]$ (1.00 g) was refluxed in *n*-octane (40 cm^3) with the appropriate arene (300 mg) for 6 h. Infrared spectroscopy indicated complete consumption of the starting material. The solvent was removed *in vacuo* and the residue separated by TLC using dichloromethane–hexane (30 : 70) as eluent. The major red-brown band was extracted and characterised in each case.

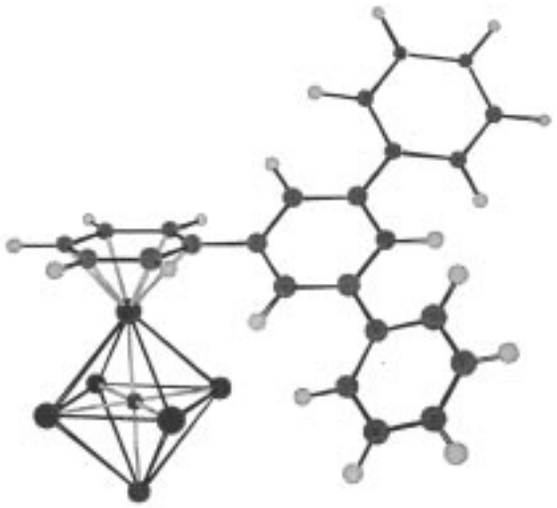

Fig. 14 Proposed molecular structure of compound **4**; the COs have been omitted for clarity

Spectroscopic data. 1a, IR (CH_2Cl_2) ν(CO) 2076m, 2034 (sh), 2025vs, 1980w, 1968w and 1812 (br) w cm^{-1}; ^{1}H NMR ($CDCl_3$) δ 7.20 (s, 4 H), 5.89 (m, 2 H), 5.69 (m, 2 H), 5.54 (m, 1 H) and 2.41 (s, 3 H); mass spectrum *m/z* 1178 (M^+) (calc. 1178); **1b**, IR (CH_2Cl_2) ν(CO) 2076m, 2034 (sh), 2025vs, 1980w, 1968w and 1812 (br) w cm^{-1}; ^{1}H NMR ($CDCl_3$) δ 7.38 (m, 3 H), 7.23 (m, 2 H), 5.94 (m, 2 H), 5.73 (m, 2 H) and 2.19 (s, 3 H); mass spectrum *m/z* 1178 (M^+) (calc. 1178); **2a**, IR (CH_2Cl_2) ν(CO) 2075m, 2068m, 2047 (sh), 2035 (sh), 2025vs, 2004w, 1985w, 1968w and 1816 (br) w cm^{-1}; ^{1}H NMR ($CDCl_3$) δ 7.22 (s, 4 H), 5.92 (m, 2 H), 5.69 (m, 2 H), 5.57 (m, 1 H), 2.71 (q, 2 H) and 1.26 (t, 3 H); mass spectrum *m/z* 1193 (M^+) (calc. 1193); **2b**, IR (CH_2Cl_2) ν(CO) 2075m, 2068m, 2047 (sh), 2035 (sh), 2025vs, 2004w, 1985w, 1968w and 1816 (br) w cm^{-1}; ^{1}H NMR ($CDCl_3$) δ 7.39 (m, 3 H), 7.22 (m, 2 H), 5.94 (m, 2 H), 5.72 (m, 2 H), 2.21 (q, 2 H) and 0.87 (t, 3 H); mass spectrum *m/z* 1193 (M^+) (calc. 1193); **3**, IR (CH_2Cl_2) ν(CO) 2076m, 2054s, 2035 (sh), 2025vs, 2002m, 1971w and 1882 (br) w cm^{-1}; ^{1}H NMR ($CDCl_3$) δ 7.64 (m, 4 H), 7.42 (m, 5 H), 5.96 (m, 2 H), 5.71 (m, 2 H) and 5.57 (m, 1 H); mass spectrum *m/z* 1242 (M^+) (calc. 1241); **4**, IR (CH_2Cl_2) ν(CO) 2076m, 2035 (sh), 2025vs, 1968w and 1811 (br) w cm^{-1}; ^{1}H NMR ($CDCl_3$) δ 7.50 (m, 13 H), 6.09 (m, 2 H), 5.77 (m, 2 H) and 5.58 (m, 1 H); mass spectrum *m/z* 1319 (M^+) (calc. 1317).

Crystallography

Crystal data for compound 1. $C_{28}H_{12}O_{14}Ru_6$, M = 1178.80, triclinic, space group $P\bar{1}$, a = 14.166(4), b = 14.984(5), c = 15.317(5) Å, α = 95.83(3), β = 97.26(5), γ = 101.02(2), U = 3139(2) Å^3, Z = 4, D_c = 2.494 Mg m^{-3}, λ = 0.710 73 Å, T = 150(2) K, μ = 2.883 mm^{-1}.

Data were collected on a Stöe Stadi-4 four-circle diffractometer equipped with an Oxford Cryosystems low-temperature device,[8] using a crystal of dimensions 0.35 × 0.35 × 0.19 mm, mounted directly from solution, by the ω–2θ method (5 < 2θ < 45°). Of a total of 8434 reflections collected, 8177 were independent. Data were corrected for absorption using ψ scans (T_{max} = 0.236, T_{min} = 0.092). The structure was solved by direct methods (SHELXTL PLUS)[9] and refined by full-matrix least-squares analysis on F^2 with $R1$ [$F > 4\sigma(F)$] and $wR2$(all data) to 0.0359 and 0.0801, respectively. The H atoms were placed in calculated positions and allowed to refine 'riding' on their C atoms. Largest peak and hole in final difference map 1.468 and −1.179 e Å^{-3}.

Crystal data for compound 2b. $C_{30}H_{16}Cl_2O_{14}Ru_6$, $M = 1277.72$, monoclinic, space group $C2/c$, $a = 27.916(2)$, $b = 19.111(2)$, $c = 14.445(11)$, $\beta = 111.224(7)°$, $U = 7184(6)$ Å^3, $Z = 8$, $D_c = 2.337$ Mg m^{-3}, $\lambda = 0.710\,73$ Å, $T = 150(2)$ K, $\mu = 2.672$ mm^{-1}.

Data were collected as above using a crystal of dimensions 0.14 × 0.20 × 0.12 mm, mounted directly from solution, by the ω–2θ method ($5 < 2\theta < 50°$). Of a total of 6239 reflections collected, 6050 were independent. Data were corrected for absorption using ψ scans ($T_{max} = 0.388$, $T_{min} = 0.061$). The structure was solved as above with $R1$ and $wR2$ 0.0526 and 0.1786, respectively. The H atoms were treated as for **1**. Modelling of a disordered dichloromethane solvate molecule was partially successful based on the two chlorine atoms only. Largest peak and hole in final difference map +1.869 and −1.796 e Å^{-3}.

CCDC reference number 186/622.

References

1 A. J. Blake, P. J. Dyson, B. F. G. Johnson, D. Reed and D. S. Shephard, *J. Chem. Soc., Dalton Trans.*, 1995, 843.
2 B. F. G. Johnson, R. D. Johnson, J. Lewis and B. H. Robinson, *J. Chem. Soc.*, 1968, 2856.
3 D. Braga, P. J. Dyson, F. Grepioni, B. F. G. Johnson and M. J. Calhorda, *Inorg. Chem.*, 1994, **33**, 3218.
4 D. Braga, P. J. Dyson, F. Grepioni and B. F. G. Johnson, *Chem. Rev.*, 1994, **94**, 1585 and refs. therein.
5 C. A. Hunter, *Chem. Soc. Rev.*, 1994, 101.
6 T. Borchert, J. Lewis, H. Pritzkow, P. R. Raithby and H. Wadepohl, *J. Chem. Soc., Dalton Trans.*, 1995, 1061.
7 J. N. Nicholls, M. D. Vargas, J. Hriljac and M. Sailor, *Inorg. Synth.*, 1989, **28**, 280.
8 J. Cosier and A. M. Glazer, *J. Appl. Crystallogr.*, 1986, **19**, 105.
9 G. M. Sheldrick, SHELXTL PLUS, Siemens Analytical Instruments, Madison, WI, 1990.

Received 29*th January* 1997; *Paper* 7/00679I